XI International Conference on Computational Plasticity. Fundamentals and Applications
COMPLAS XI
E. Oñate, D.R.J. Owen, D. Peric and B. Suárez (Eds)

SOLDIER PILE WALLS – 3D NUMERICAL ANALYSIS OF SOLDIER PILE EMBEDMENT

CHALMOVSKY, J., FIALA, R. AND MICA, L*

* Faculty of Civil Engineering, Department Geotechnics
Brno University of Technology
Veveri 95, 602 00 Brno, Czech Republic
e-mail: chalmovsky.j@fce.vutbr.cz

Key words: 3D Passive Earth Pressure, Soldier Pile, Numerical Modeling.

Abstract. The paper is focused to a determination of spatial passive earth pressure (soil resistance) in the embedded part of the soldier pile. The analysis of 3D passive earth pressure is done numerically in software Plaxis 3D Tunnel v 2.2. The analysis of 3D passive earth pressure (soil resistance) is done for cantilever soldier pile walls in sand. The parameters for constitutive models were calibrated based on laboratory tests (triaxial – CD and oedometric tests). Hardening soil model is used in analysis. Outputs of the numerical analysis present a comparison for the resulting passive earth force in case of different *b/d* ratios and different angles of internal friction, parameter ω_R which is used in approach by Weissenbach and finally the magnitude of 3D passive earth pressure coefficients ($K_{P,3D}$) for different soldier pile distance (L), embedment depth (d) and angles of internal friction (φ'). Numerical analysis showed that the 3D passive earth pressure is higher than currently presented approach by Weissenbach. The other present theories don't take to account the behaviour for higher slenderness ratio and influence adjacent soldier pile no way.

1 INTRODUCTION

Passive earth pressure analysis plays an important role in geotechnical design process. Primarily, it is a spatial effect which is significant for local structural elements analysis (for example soldier pile, piles with long axial distances etc.) and therefore it might be important for designers and engineers to gain new knowledge and information about this problem. The topic of spatial passive earth pressure has been analysed by various authors who used three different methods: the limit equilibrium method, the slipe-line method and the limit analysis method. The first mentioned method is used by Blum [2] for analysing the 3D passive earth pressure. The resulting force of passive earth pressure is defined by

$$E_{Ph,Blum} = \frac{1}{2}\gamma d^2 btg^2\left(\frac{\pi}{4}+\frac{\phi}{2}\right)+\gamma\frac{d^3}{6}tg^2\left(\frac{\pi}{4}+\frac{\phi}{2}\right) \quad (1)$$

The disadvantage of Blum solution was, that interface between soil and structural element

was neglected and also the shape of 3D wedge was simplified. The author who firstly analysed the soldier pile wall was Weissenbach [10]. Weissenbach divided relation for determination of 3D earth passive pressure to two components. The first component includes the unit soil weight and the second equation member includes the cohesion of soil. He defined parameters ω_R and ω_K, which depend on the embedment depth (d) and width (b) of structure element and angle of internal friction of soil. In 1964 Ovesen [3] performed number of test on using dense sand. He found out that 3D passive earth pressure is significantly influenced by the structure element thickness. He also found out that structural members with smaller width give significantly higher passive earth pressures than it has ever been considered.

Another theory, limit analysis applying upper bound limit theorem, is widely used for determination of 3D earth passive earth pressure in the present. This theory was firstly applied by Soubra and Regenass [6]. Their calculations were based on determination of kinematically admissible multi-block failure mechanism, which consisted of one ore more rigid blocks. The blocks were labeled as „one-block, multiblock a truncated multiblock". The last-mentioned block is based on reduction of „multiblock" mechanism. The upper bound theorem within the framework of limit analysis theory is also considered in research works done by authors Škrabl, Macuh [7], Vrecl-Kojc, Škrabl [9] and Škrabl [8]. First mentioned authors took into account rotational failure mechanism. This mechanism is bounded by logarithmic spiral in vertical section and by hyperbolic shape in plan. On the contrary, Vrecl-Kojc, Škrabl [9] continued the work of Soubra a Regennas [6], who used translational failure mechanism, and they slightly modified it. The results of this analysis showed that the passive earth pressure coefficient is lower in comparison with Soubra and Regennas. These results were also confirmed by Škrabl [8] who updated his previous model using non-linear passive earth pressure distribution on non-rigid structural element.

Previously mentioned procedures used the change of structural element width to determinate the passive earth pressure coefficients for different d/b ratio. However, this procedure is not appropriate for soldier pile walls, where the change of embedment depth is more dominant than structural element width change.

The article is focused on the analysis of passive earth pressure for geotechnical structures where 3D effect is predominant (for example: soldier beam wall – Fig. 1). The above mentioned authors determined the 3D passive earth pressure for ratio $b/d > 0{,}25$. Benmebarek *et al.* [1] used minimal *b/d* ration 0,1. In our study, ration $b/d < 0{,}14$ has been taken into account. This range of b/d ratio is more common in case of using soldier pile walls, where a soldier pile is actually a slender structural element (usually I, IPE or HEB profile). For these small rations comparison of the resulting passive earth pressure force is done. It is compared with theory of Weissenbach [10] - (2) and Blum [2] - (1).

$$E_{Ph,Weissenbach} = \frac{1}{2}\gamma\omega_R d^3 + 2\alpha\omega_K d^2 \tag{2}$$

The resulting passive earth pressure force in our study is determined from 3D numerical analysis, which is briefly described in the next chapter.

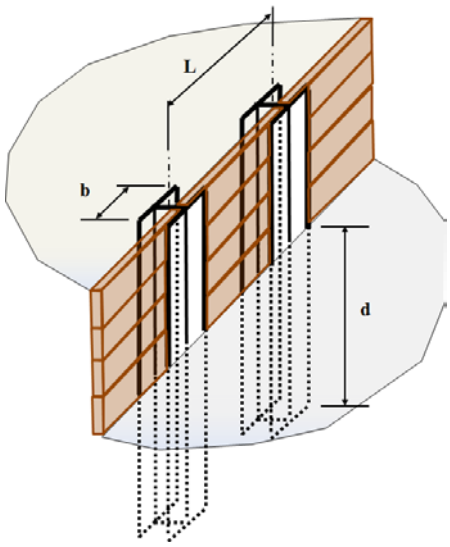

Figure 1: Scheme of soldier beam wall

2 NUMERICAL MODELS

The numerical calculations were done in software Plaxis 3D Tunel V2.4. The only one soldier pile is modelled and horizontal distance between them is done the width of model (Fig. 4). The width of soldier pile is 275 mm and it is supposed as very stiff. The soldier pile is installed in sand. The variable parameters are horizontal distance between soldier pile *L* (1; 1,5; 2; 2,5 and 3 m), embedment depth *d* (1;2;3m) and angle of internal friction φ (30°;35°;40°). The numerical analysis .The interface between soldier pile and soil is neglected in our analysis ($\delta/\varphi = 0$). The movement of soldier pile was the same longwise of embedment depth and the movement was done by function horizontal incremental. The output was resulting force of passive earth pressure which corresponded to stabilization of activation force during increasing movement of soldier pile.

2.1 Input parameters

Numerical modelling has been carried out in sand and for the description of the soil the Hardening soil model – HS (Fig. 2) has been used. The sand was classified according to EN ISO 14688-1 as "Sa". The void ratio was e = 0.524 in the natural state [11]. The sample was taken to conduct an extensive and complex laboratory tests to determine the input parameters for selected constitutive models. Oedometer, shear box and triaxial (CD test) test were performed on the samples. Oedometer test was used to determination of modulus E_{oed}^{ref} for HS model with the reference stress p_{ref} = 100 kPa. The result from oedometer and its calibration of HS model is shown in Fig. 3a. Angle of friction φ_{ef} and the cohesion c_{ef} were determined from shear box test. Triaxial CD test was used to determination of reference modulus E_{50}^{ref} and E_{ur}^{ref} for HS model with the reference stress p_{ref} = 100 kPa. In order to determine E_{ur}^{ref} parameter, unloading of the sample was carried out. Figure 3b shows stress-strain diagram from experiment (blue line) and calibrated stress – strain diagram with usage HS model. The laboratory tests were done in the geotechnical laboratory of the Faculty of Civil Engineering, Brno University of Technology.

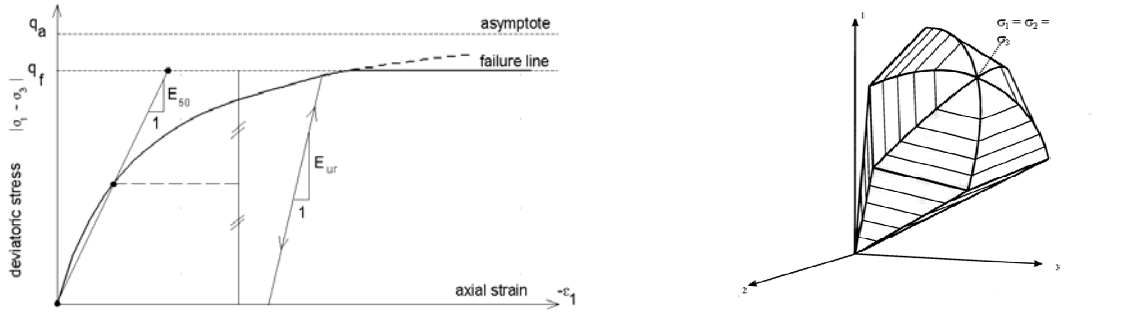

a) Hyperbolic stress-strain relation b) Soil plasticity surface for cohesionless soil

Figure 2: Hardening soil model [4]

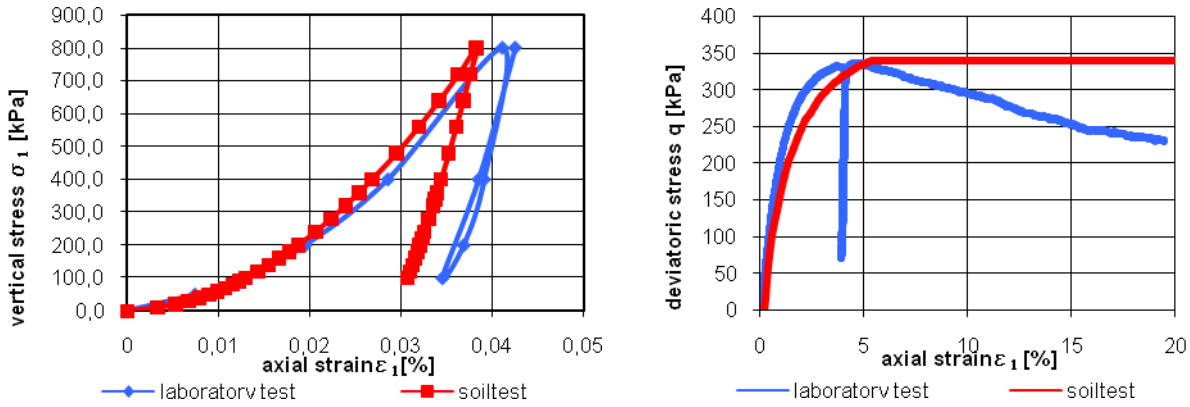

a) Oedometer test - stress-strain diagram b) Triaxial test - stress-strain diagram

Figure 3: Laboratory test and calibration

The input parameters for Hs model are summarized in Table 1.

Table 1: Input parameters for sand

γ_{unsat}	E_{50}^{ref}	E_{oed}^{ref}	E_{ur}^{ref}	m	c´	φ´	ν_{ur}	R_f	p_{ref}
[kN/m^3]	[MPa]	[MPa]	[MPa]	[-]	[kPa]	[°]	[-]	[-]	[kPa]
17,6	22,567	11,22	59,14	0,50	0,1	40	0,2	0,8	100

2.2 Description of numerical calculations

For 2D calculations the plane strain condition is considered. General tensor of proportional deformations consists of 6 terms (3) in plane by equitation (4) reduce to triple tensor (5).

$$\underline{\varepsilon}_{3D}^{T} = \left\{ \varepsilon_{xx}; \varepsilon_{yy}; \varepsilon_{zz}; \gamma_{xy}; \gamma_{yz}; \gamma_{xz} \right\} \tag{3}$$

$$\varepsilon_{zz} = -\frac{\partial w}{\partial z} = 0\,;\ \gamma_{yz} = -\frac{\partial w}{\partial y} - \frac{\partial v}{\partial z} = 0\,;\ \gamma_{xz} = -\frac{\partial w}{\partial x} - \frac{\partial u}{\partial z} = 0 \tag{4}$$

$$\underline{\varepsilon}_{2D}^{T} = \left\{ \varepsilon_{xx}; \varepsilon_{yy}; \gamma_{xy} \right\} \tag{5}$$

The restrction of the deformation in the plane of retaining system cannot take into account

spatial character of the earth pressure under the bottom of the excavation with limited effective width. It leads to the conservative calculation of the passive earth pressure which can flow into non-economic design of such a retaining structure. For the purpose of examination of the passive earth pressure redistribution under the bottom of the excavation, the software Plaxis 3D Tunel v 2.2 has been used. For the example analysis the cut-out from the excavation pit with the high of 4m has been modelled. The example has been modelled as symmetrical with the axis in the middle distance between the soldier piles. The soldier piles have been embedded 2m, 3m and 4m under the bottom of the excavation. The distance of the soldier piles in the spatial analysis has been 1,0m; 1,5m; 2,0m; 2,5m and 3,0m. The soldier pile has been modelled as stiff element with the plan dimensions 275x275mm. The dimensions of 3D models are 10,25m (high), 13,5m (depth) and width is variable. The number of elements varies from 6030 to 7596. In the calculations only a part under the bottom of the excavation has been modelled mainly because of the time savings. The part above the bottom of the excavation has been substituted by equivalent geostatic stress. When considering the excavation pit 4m high and the bulk density 20kN/m^3 of the soil above the bottom, the upper edge of the models has been loaded by the distributed load of 80kPa. Figure 4 represent 3D model with the distance of the soldier piles 3,0m and the embedded depth of 4,0m.

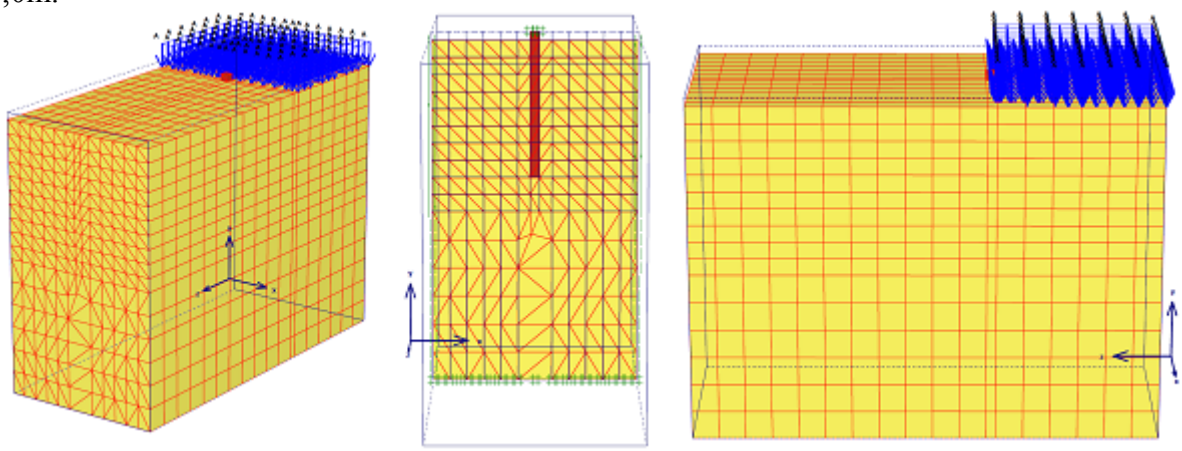

Figure 4: Different views on numerical models

In order to mobilise passive earth pressure the soldier pile has been subjected to prescribe deformation. This prescribe load has been increasing until the steady state of the passive force. The construction staged are summarised in Table 2.

Table 2: Construction sequences

ID	Name of Stage	Note
1	Initial conditions	For simulation of geostatic stress above the bottom of excavation POP=80kPa
2	Soldier Pile Construction	Staged construction
3	Primary prescribe deformation – 5mm	Staged construction
4	Increasing of prescribe deformation	Staged construction - incremental multipliers, M_{disp}=2,0

The variations of the calculations in the parametrical studies are summarised in the Tab. 3.

Table 3: Description of performed calculations

ID-3D	φ´ (°)	*L* (m)	*t* (m)
1a; 1b; 1c	30,35,40	1,00	2,00
2a; 2b; 2c	30,35,40	1,00	3,00
3a; 3b; 3c	30,35,40	1,00	4,00
4a; 4b; 4c	30,35,40	1,50	2,00
5a; 5b; 5c	30,35,40	1,50	3,00
6a; 6b; 6c	30,35,40	1,50	4,00
7a; 7b; 7c	30,35,40	2,00	2,00
8a; 8b; 8c	30,35,40	2,00	3,00
9a; 9b; 9c	30,35,40	2,00	4,00
10a; 10b; 10c	30,35,40	2,50	2,00
11a; 11b; 11c	30,35,40	2,50	3,00
12a; 12b; 12c	30,35,40	2,50	4,00
13a; 13b; 13c	30,35,40	3,00	2,00
14a; 14b; 14c	30,35,40	3,00	3,00
15a; 15b; 15c	30,35,40	3,00	4,00

3 RESULTS AND DISCUSSION

In the previous studies and analysis, primarily, small slenderness ratios were taken into account and the interaction between the adjacent structural elements was not considered (Fig. 5). The objective of the performed numerical analysis in this study was to investigate just the range of higher slenderness. Blum approach [2], Weissenbach approach [10] and partially Benmebarek *et al.* [1] should be used for comparisons because their researches partially covers the range of higher slenderness, but still without taking into account the interaction between the adjacent passive wedges. Only exception is the theory derived by Weissenbach which is used in German standard in order to design the soldier beam walls.

In the first step, the comparisons for the resulting passive earth force E_{ph} in case of different *b/d* ratios and different angles of internal friction were done (Fig. 6÷8). The numerically determined values of E_{ph} forces are then compared with resulting passive forces calculated by Weissenbach approach [10]. The values of E_{ph} forces are calculated for two cases. Firstly, the adjacent passive wedges overlap each other (6a). Secondly, the adjacent passive wedges do not overlap each other (6b). The value of E_{ph} (1) force calculated by Blum [2] is also shown in the graphs.

$$\mathrm{L} < 0{,}5\mathrm{d} \ \wedge \ \delta = 0 \Rightarrow E_{ph} = \frac{1}{2} \cdot \gamma \cdot \omega_{ph} \cdot L \cdot d^2 \quad \wedge \quad c = 0 \quad \Rightarrow \quad \omega_{ph} = K_{ph} \tag{6a}$$

$$\mathrm{L} \geq 0{,}5\mathrm{d} \ \wedge \ \delta = 0 \Rightarrow E_{ph} = \frac{1}{2} \cdot \gamma \cdot \omega_{r} \cdot d^3 \quad \wedge \quad c = 0 \quad \wedge \quad \omega_R [5] \tag{6b}$$

The analysis confirmed that the effect of adjacent elements is not negligible. It is apparent from the results that the increase of soldier pile distance for constant *b/d* ratio causes also the passive earth force increase. This tendency is related to the overlapping of passive wedges for the case of small soldier pile distances *L*. The results also showed rapid rise in passive force for lower *b/d* ratio. There is a reasonable consistency in resulting forces between computed results and results according to Weissenbach [10]. Blum [2] indicates lower forces values in contrary to the numerical results. It is probably caused by the fact that the simplified passive

wedge geometry is used in Blum solution.

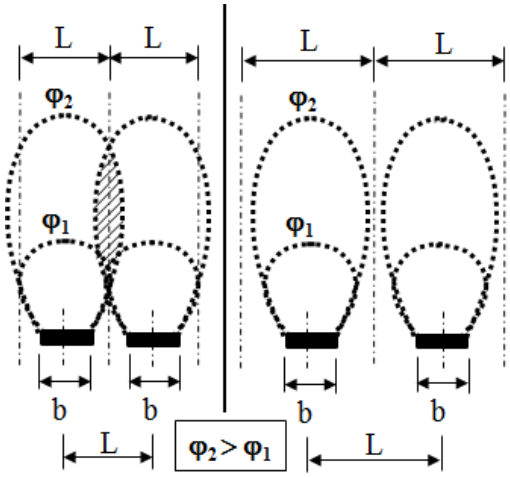

Figure 5: Scheme - influence of adjacent passive wedges

In the second step we focused on the parameter ω_R determination which used Weissenbach in his approach in order to affect spatial character of the passive earth pressure in case of analysing the constructions with limited width. This parameter was derived from (6a and 6b) where numerically calculated value of E_{ph} was substitute to the left part of the equation. Zero cohesion was assumed in soil parameters; the second equation member is therefore equals to zero. The numerically determined values of ω_R coefficient were compared again with values according to Weissenbach (Fig. 9÷11). It is apparent form the results that the ω_R values are directly proportional to the soldier pile distance, which confirms previous statement that the passive earth force is directly proportional to the soldier pile distance. The numerically determined values of ω_R are higher in comparisons with values by Weissenbach. These difference results in higher passive earth forces in case of FEM analysis. This tendency is even more evident for higher *b/d* ratio.

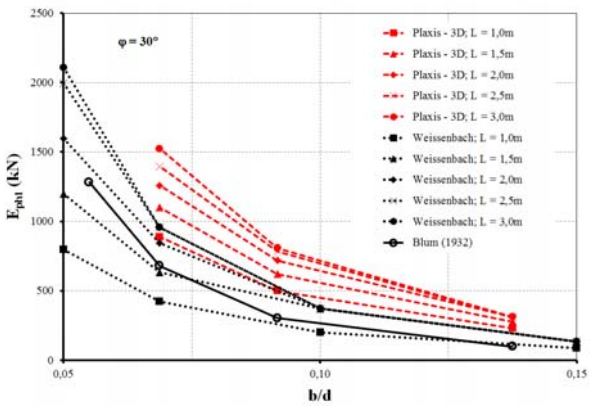

Figure 6: Comparison of E_{ph} with Weissenbach and Blum for φ = 30° and δ/φ = 0° for different values of b/d ratio.

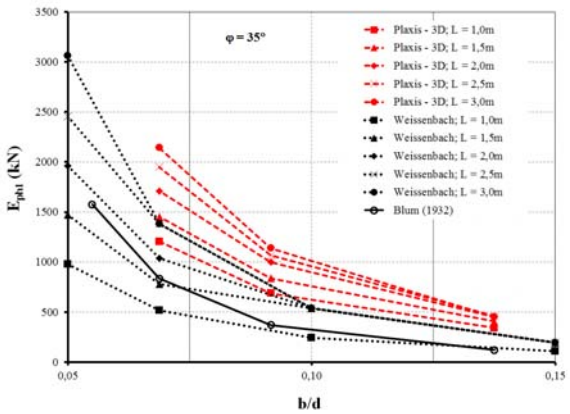

Figure 7: Comparison of E_{ph} with Weissenbach and Blum for φ = 35° and δ/φ = 0° for different values of b/d ratio.

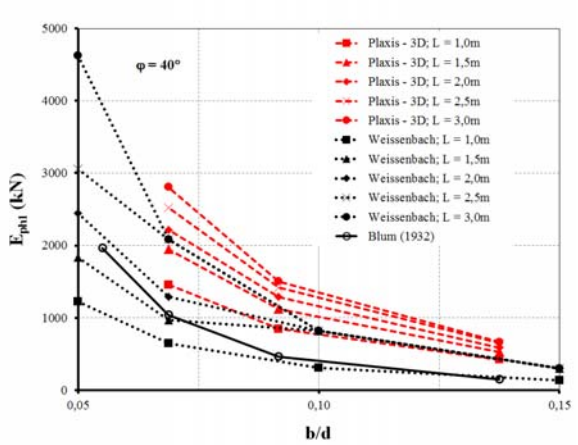

Figure 8: Comparison of E_{ph} with Weissenbach and Blum for φ = 40° and δ/φ = 0° for different values of b/d ratio.

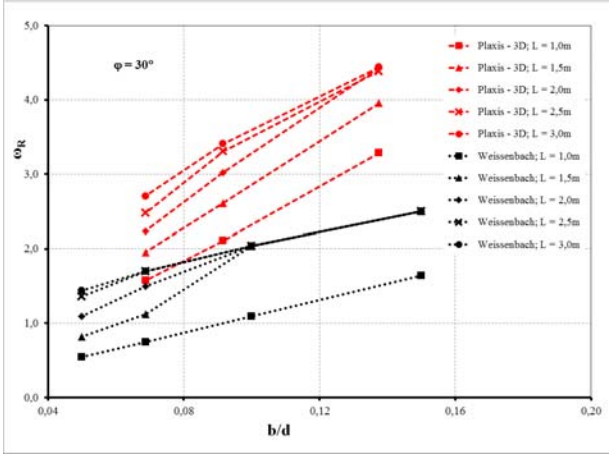

Figure 9: Comparison of ω_R with Weissenbach and Blum for φ = 30° and δ/φ = 0° for different values of b/d ratio.

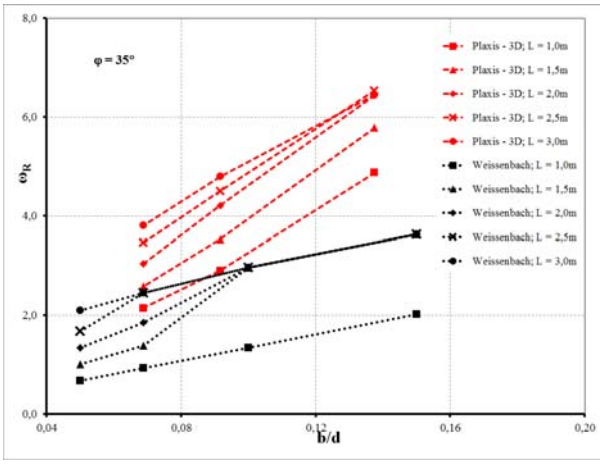

Figure 20: Comparison of ω_R with Weissenbach and Blum for φ = 35° and δ/φ = 0° for different values of b/d ratio.

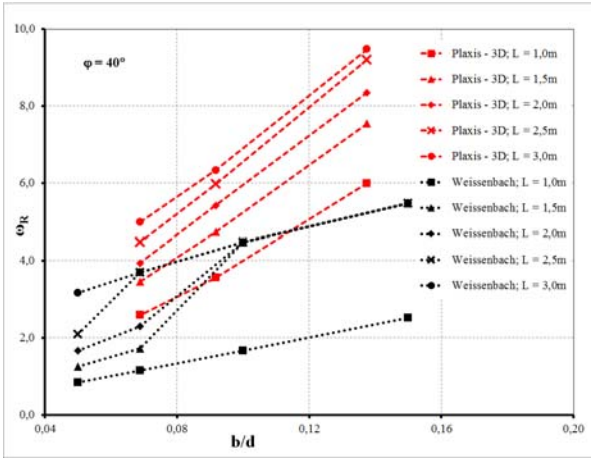

Figure 31: Comparison of ω_R with Weissenbach and Blum for φ = 40° and δ/φ = 0° for different values of b/d ratio.

The last step of the analysis was determination of 3D passive earth pressure coefficients ($K_{P,3D}$) for different soldier pile distance (L), embedment depth (d) and angles of internal friction (φ'). Using $K_{P,3D}$ (7) coefficients instead of ω_r might by also the way how to involve the spatial effect in 2D solution.

$$E_{ph} = \frac{1}{2} \times \gamma \times d^2 \times b \times K_{p,3D}$$
$$K_{p,3D} = \frac{2 \times E_{ph}}{\gamma \times d^2 \times b} \quad (7)$$

The computed values of passive earth coefficient $K_{P,3D}$ are listed in Table 4. The table shows that the passive earth pressure coefficient value are not only depended on distance L and angle of internal friction φ', but also on the embedment depth d. For large values of embedment

length *d*, the 3D effect decrease the value of $K_{P,3D}$ for small distances *L*. The rate of decreasing is also affected by angle of internal friction φ. Note: In all presented analysis is values of soil-wall interface friction $\delta/\varphi = 0°$.

Table 4: $K_{p,3D}$ coefficient

b/d	φ	L				
		1	1,5	2	2,5	3
0,07	30°	22,92	28,41	32,52	36,04	39,34
	35°	31,18	37,57	44,18	50,33	55,35
	40°	37,64	50,33	57,24	65,10	72,51
0,09	30°	22,99	28,48	32,96	36,07	37,15
	35°	31,58	38,54	45,93	49,04	52,30
	40°	38,86	51,67	59,11	65,15	69,10
0,14	30°	23,90	28,76	32,21	31,90	32,28
	35°	35,43	42,02	46,79	47,49	46,86
	40°	43,61	54,88	60,72	66,94	68,93

4 SUMMARY AND CONCLUSIONS

Set of 3D numerical models were created in order to analyse the distribution of passive earth pressures behind the soldier pile wall, which is a truly spatial phenomenon. Parallel horizontal prescribed displacement with no rotation was applied on the soldier pile. Soldier pile was modelled as a rigid member. The interface elements were not used. The FEM calculation results are presented in form of passive earth forces.

The passive earth pressure increase with increasing soldier pile distance. This is due to the passive wedges overlapping. Passive earth force also grows exponentially with increasing slenderness. Calculated forces are in reasonable match with Weissenbach [10]. Blum [2] indicates lower forces values in contrary to the numerical results.

Numerical analysis have showed, that the coefficients ω_R respectively ω_{ph} are directly proportional to the soldier pile distance, which is in agreement with Weissenbach, however Weissenbach underestimates the ω_R respectively ω_{ph} values in comparisons to the numerical results. The differences are bigger for higher values of slenderness.

Final part of the article was focused on comparison of passive earth pressure coefficients K_{p3D} for different soldier pile distances and embedment length. It is obvious from the result that coefficient K_{p3D} is directly proportional to the soldier pile distance. The differences are, however, smaller for bigger soldier pile distances, because of the fact, that passive wedges doesn´t influence each other for bigger distances and they start to be independent on soldier pile distance.

For further research, parametric study with non-zero soil-wall friction angles, with another type of deformation (rotation) and also with considering non-rigid soldier pile will be undertaken. Spatial passive earth pressure for cohesive soils will be also analysed.

AKNOWLEDGMENT

This contribution was financially supported by the project of the Czech Science Foundation (GA ČR) No. GA103/09/1262, by the research project of The Ministry of

Education, Youth and Sports (MŠMT ČR) No. MSM0021630519 and by the project FAST-S-11-39. Authors appreciate this support.

REFERENCES

[1] Benmebarek, S., Khelifa, T., Benmebarek, N. and Kastner, R. Numerical evaluation of 3D passive earth pressure coefficients for retaining wall subjected to translation. *Computers and Geotechnice* (2008) **35**:47-60.

[2] Blum, H. Wirtschaftliche Dalbenformen und deren Berechnung. *Bautechnik* (1932) **10(5)**:122-135.

[3] Ovesen, N. K. *Anchor slabs, calculation method, and model tests*. Danish Geotechnical Institute, Kopenhagen (1964).

[4] Schanz, T., Vermeer, P.A., Bonnier, P.G. *The hardening soil model: Formulation and Verification*, Beyond 2000 in Computional Geotechnics – 10 Years of Plaxis, Rotterdam (1999)

[5] Smoltczyk, U. *Grundbau-Taschenbuch, Teil3: Gründungen*. Ernst & Son, (2001).

[6] Soubra, A.-H. and Regennas, P. Three-dimensional passive earth pressures by kinematical approach. *Journal of Geotechnical and Geoenvironmental Engineering*. ASCE, (2000) **126**(11):969-978.

[7] Škrabl, S. and Macuh, B. (2005). Upper-bound solution of three-dimensional passive earth pressures. *Canadian Geotechnical Journal* (2005) **42**:1449-1460.

[8] Škrabl, S. The limit values and the distribution of three-dimensional passive earth pressure. *Acta geotechnica Slovenika* (2008) **1**:21-34.

[9] Vrecl-Kojc, H. and Škrabl, S. (2007). Determination of passive earth pressure usány three-dimensional failure mechanism. *Acta Geotechnica Slovenika* (2007) **4**(1):11-23.

[10] Weissenbach, A. *Der erdwiderstand vor schmalen druckflechen*. PhD thesis, Franzius Institut für Grund und Wasserbau der Technischen Hoschule, Hannover (1961).

[11] Zedník, J. Zajištení stavební jámy v píscích. *Master thesis*, VUT Brno: 2010. (in Czech)

SYMBOLS

b ...	Width of soldier pile (m)
c ...	Cohesion, effective (kPa)
d ...	Eembedment depth (m)
E_{oed}^{ref} ...	Tangent stiffness for primary oedometer loading (kPa)
E_{50}^{ref} ...	Secant stiffness in standard drained triaxial test (kPa)
E_{ur}^{ref} ...	Unloading/reloading stiffness (kPa)
E_{ph} ...	Resulting passive earth pressure force (kN)
$K_{P,3D}$ ...	3D passive earth pressure coefficients
L ...	Horizontal distance of soldier pile (m)
m ...	Power for stress-level dependency of stiffness (-)
R_f ...	Failure ratio (-)
γ ...	Unit weight of soil (kNm^{-3})
φ ...	Angle of internal friction, effective (°)
ν_{ur} ...	Poisson´s ratio for unloading-reloading (-)
ω_R/ω_{ph}...	Coefficient by Weissenbach